Tom Milligan
Milligan & Associates
8204 West Polk Place
Littleton, CO 80123
(303) 977-7268
(303) 977-8853 (Fax)
Tmilligan@compuserve.com (e-mail)

Editor's introduction

My fax number has changed to (303) 977-8853, and I decided that a commercial e-mail provider will remain more constant. My e-mail address is TMilligan@compuserve.com.

A few days after the October, 1996, column appeared, I received the following comment from Mike Francis at NIST. His comments made me re-think about sampling, and near-field measurements in general. In the past few months, we have traded correspondence and collaborated on this and other papers. This interchange has increased my knowledge of the subject, and I want to share Mike's comments and our further investigations with the readers. Thanks to Mike for clarifying this topic, which touches both the near-field measurement and the analysis of apertures. In my reply, I show that the errors are predictable, and depend on the edge condition of the aperture. It is possible to extend the sampling of apertures to the errors of numerical integration of an aperture, using either the trapezoidal or Simpson's rule. The errors have a predictable distribution, which depends on the aperture edge condition, because numerical integration is a weighted sampling.

Aperture-Sampling Requirements

Michael H. Francis
Antenna and Materials Metrology Group
National Institute of Standards and Technology
Boulder, Colorado

Regarding your recent article, "Aperture-Sampling Requirements in Planar Near-Field and Pattern Calculations," in the October, 1996, AP *Magazine*, I would like to point out some shortcomings in the nomograph (and equations?) when aliasing errors are significant.

I believe the nomograph relating sampling increment and maximum pattern angle can be derived from the discrete Fourier transform equation that relates the spacing in Fourier space to the spacing in normal space, as follows:

$$\delta k_x = \frac{2\pi}{N\delta_x}, \tag{1}$$

where δk_x is the spacing in Fourier space, δ_x is the sample spacing in the near field, and N is the total number of data points. Also,

$$k = \frac{2\pi}{\lambda},$$

and

$$\sin\theta = \frac{k_x}{k}. \tag{2}$$

From these, it follows that the maximum angle of coverage is

$$\sin\theta_{max} = \frac{k_{xmax}}{k} = \frac{N\delta k_x}{2k} = \frac{\lambda}{2\delta_x}. \tag{3}$$

Thus, the equations for the nomograph are

$$\theta_{max} = \sin^{-1}\left(\frac{\lambda}{2\delta_x}\right)$$

and

$$\delta_x = \frac{\lambda}{2\sin\theta_{max}}. \tag{4}$$

While these equations give the angle of coverage of the data, based on the sampling alone, a portion of this pattern contains aliasing errors. The discrete Fourier transform is a periodic continuation of the spectrum in Fourier space. Figure 1 is the periodic continuation for the case without aliasing, and satisfies the sampling-theorem criterion that we must have at least two samples per period. Figure 2 (Figure 6 of [1]) is for the case where the sampling theorem is

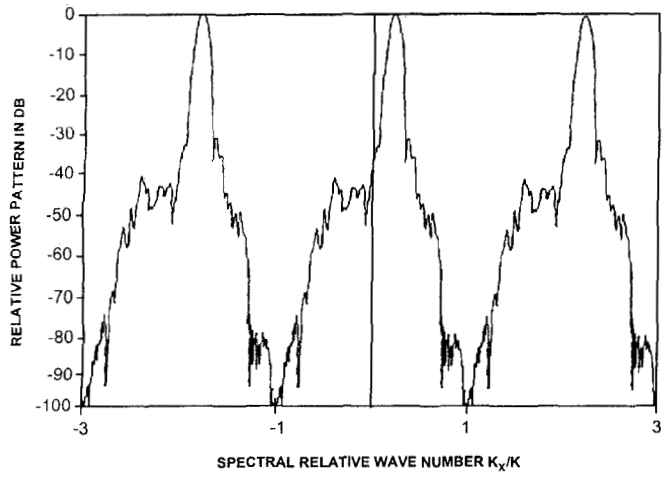

Figure 1. An illustration of the periodic continuation of the spectrum in Fourier space without aliasing when the sampling theorem is satisfied: $k_x = k$, $\delta_x = \lambda/2$ [1].

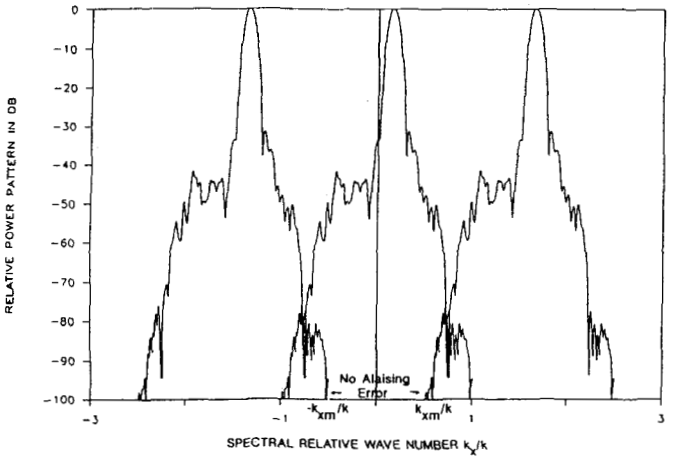

Figure 2. When the sampling theorem is not satisfied, the periodically continued patterns begin to overlap: $k_x < k$, $\delta_x > \lambda/2$ [1].

not satisfied. We see that the periodically continued patterns begin to overlap.

In this overlap region, the measured result will equal the complex sum of the overlapping patterns. For example, if the pattern is symmetric in amplitude and phase, then at the point θ_{max}, the measured pattern will have an amplitude that is twice the correct value. For a highly directive antenna, the errors in the overlap region may occur below the accurate measurement threshold; however, for a broad-beam antenna, the errors may be significant.

If the probe-test-antenna separation distance is sufficiently large, the effect of the non-propagating (evanescent) modes will be negligible (below -60 dB). If the entire pattern in the forward direction is significant, then for sampling that provides pattern information to $\sin\theta_{max} = (k_{max}/k) = 1 - \Delta$, aliasing will extend to. The portion of the pattern where the aliasing is negligible is then defined by

$$\frac{k'_{max}}{k} = \frac{2k_{max}}{k} - 1 = \frac{\lambda}{\delta_x} - 1. \tag{5}$$

Thus, the sampling requirement for negligible aliasing is [1, Equation (47)]

$$\delta_x = \frac{\lambda}{1 + \left(\frac{k'_{max}}{k}\right)}. \tag{6}$$

The sampling requirement and the maximum pattern coverage are then related by

$$\theta'_{max} = \sin^{-1}\left(\frac{\lambda}{\delta_x} - 1\right)$$

and (7)

$$\delta_x = \frac{\lambda}{1 + \sin\theta'_{max}}.$$

Equation (7) is more restrictive than Equation (4). Equation (4) and the nomograph imply that the sampling must be λ to obtain coverage to an angle of 30°. However, Equation (7) implies that for the pattern at 30° to have negligible aliasing errors, the sampling must be $2\lambda/3$. Even at 0°, Equation (7) implies a sampling criterion of λ for the pattern to have negligible aliasing errors.

Some measurement errors can give the appearance of significant energy in non-propagating modes, which can alias back into the pattern. For example, if the test antenna has periodic structures (like a phased array), the probe-test-antenna multiple reflections may cause high-frequency spatial variations that alias into the pattern. In such a case, requirements will be even more severe that Equation (7).

Reference

1. A. C. Newell, "Error Analysis Techniques for Planar Near-Field Measurements," *IEEE Transactions on Antennas and Propagation*, **AP-36**, June 1988, pp. 754-768.

Author's (Editor's) Reply

Michael Francis has some very interesting comments. To match the original article, Equation (7) was reduced to a nomograph, shown in Figure 3. It places severe requirements on planar near-field measurements. The problem, he points out, is that the original nomograph only gives the angle where the pattern due to sampling folds over and repeats. There is significant error at this angle. These comments led to a study of sampling errors that could be fit to a unified theory for linear aperture distributions. We do not normally sample as closely as stated by Equation (7) in near-field measurements, but we need to know what errors to expect for coarser measurements.

Figure 4 shows the pattern for a linear Taylor aperture distribution, designed for 30 dB sidelobes (the dark curve), along with the pattern from a sampling of the aperture (light curve). The

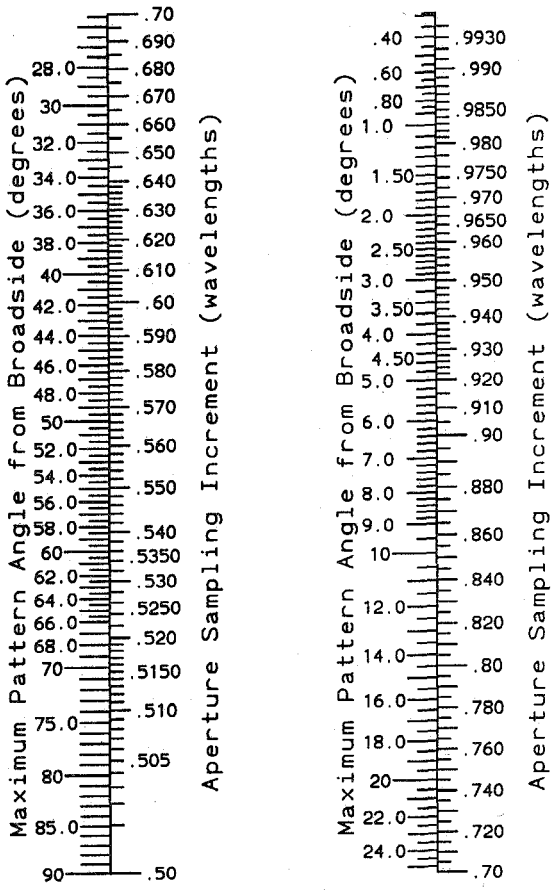

Figure 3. A nomograph for Equation (7), relating the maximum pattern coverage to the sampling requirement.

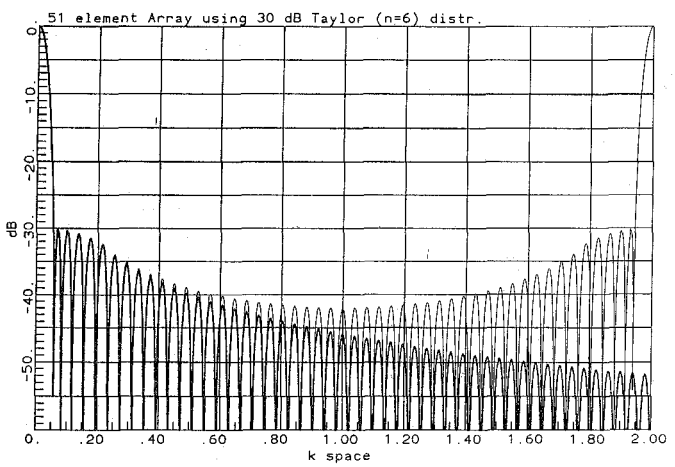

Figure 4. The pattern for a linear Taylor aperture distribution, designed for 30 dB sidelobes (dark curve), and a sampling of the aperture (light curve). The abscissa is $\sin\theta$. Note that the pattern calculated from the sampled distribution always exceeds the continuous aperture pattern.

abscissa of the curve is $\sin\theta$ (k-space). Remember that the Taylor distribution has a step discontinuity at the edge of the distribution. The pattern produced from the sampled distribution repeats at even integers of $\sin\theta$, because the sampling interval is $\lambda/2$, in this case. Figure 4 shows that the pattern calculated from the sampled distribution always exceeds the continuous aperture pattern. When the analysis is repeated with a uniform distribution, we get the same error distribution. But then, the Taylor distribution is only a modification of the uniform distribution. If we increase the sampling to λ, the response repeats at integer intervals, with the fold-over at $\sin\theta = 0.5$ (30°), as shown in Figure 5. A comparison between Figures 4 and 5 shows that the error is the same in both figures, when we start at the fold-over point and move toward zero. Further analysis showed that the result is independent of the number of sampling points, when the array and the aperture size is increased to match the number of points.

The aperture edge taper determines the rate of decrease of the far sidelobes [1]. To determine the effect of edge taper, a distribution with a linear slope at the edge was considered. Figure 6 shows the patterns from a continuous aperture and a sampled aperture for a Taylor distribution with an edge null [2], a modification of the cosine distribution. At all points, the sampled-distribution pattern (light curve) lies below the aperture-distribution pattern (thick curve). The magnitude of the error is larger for this case than for a distribution with a step discontinuity on the edge. The grating lobe, and its sidelobes due to the sampling, are out-of-phase with the primary pattern (centered at zero), and produce a null. Figure 7

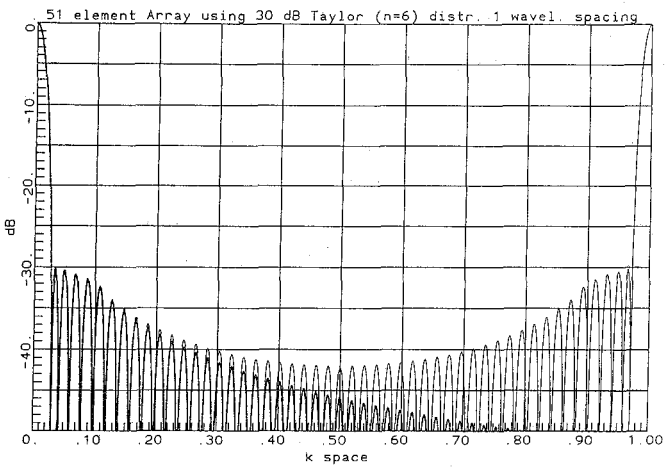

Figure 5. The patterns of Figure 4, with a sampling interval of λ.

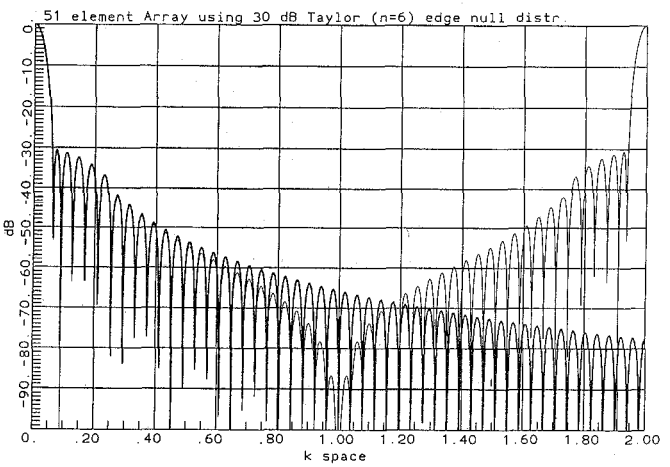

Figure 6. The patterns from a continuous aperture (dark curve) and a sampled aperture (light curve) for a Taylor distribution with an edge null [2].

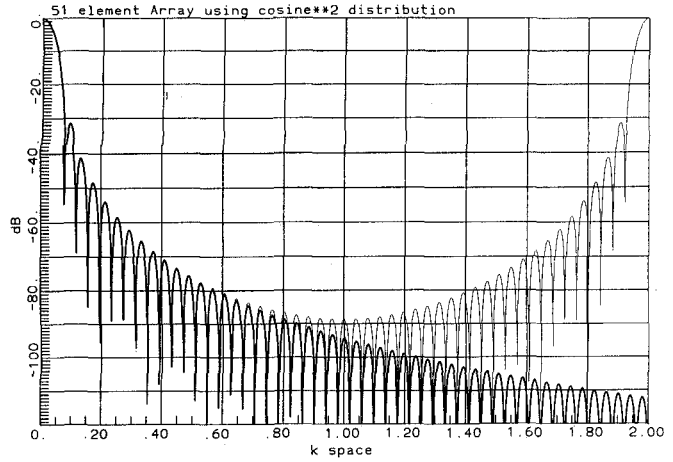

Figure 7. The continuous (dark curve) and sampled (light curve) patterns for a cosine-squared aperture distribution, with zero derivative on the edge of the aperture.

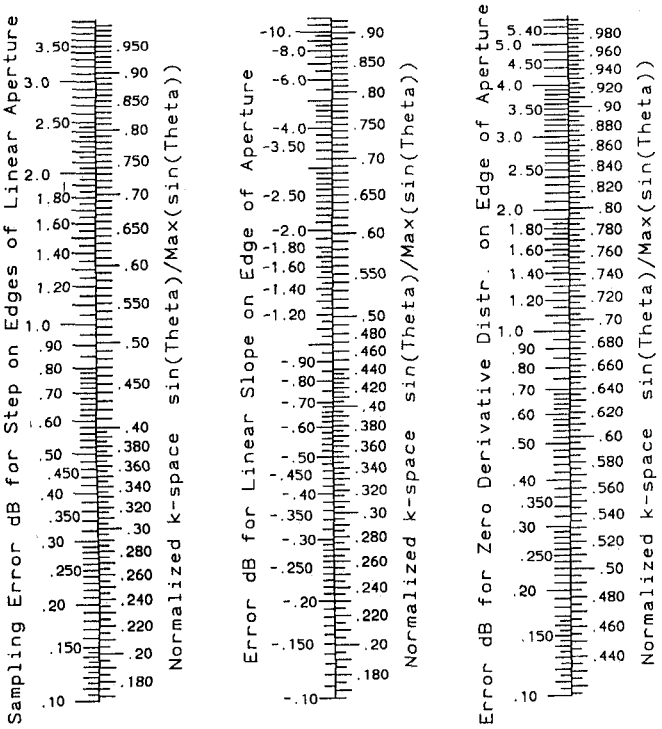

Figure 8. A nomograph giving the sampling error for the aperture distributions shown in Figures 4, 6, and 7.

continues the development by giving the patterns for a cosine-squared aperture distribution, which has a zero derivative at the edge of the distribution. The sampling response (light curve) is always greater than the pattern of the aperture distribution (thick curve). The error decreases more rapidly when we move along the pattern to the left, from the fold-over point at $\sin\theta = 1$, when compared to the distribution with a step discontinuity on the edge. The slope of the aperture-distribution pattern is greater at the fold-over point, and produces less error in the sampled response.

Figures 4 and 5 show that the error is proportional to the distance from the fold-over point in k-space. Figure 8 uses this idea in a nomograph that gives the error for the three cases considered. Analysis of a number of other distributions showed that aperture distributions with the same edge characteristics have the same error. This fold-over point is determined by the original nomograph, or by Equation (4).

Consider the example where the Newell equation result is a $2\lambda/3$ sampling for patterns to 30°. Using Equation (4) produces a fold-over point of 3/4. The normalized k-space point for 30° is 0.5/0.75 or 2/3. The scales on Figure 8 give errors of 1.65 dB for a linear aperture distribution with an edge step; -2.7 dB for a linear edge slope to zero; and 0.85 dB for an aperture with a zero slope at the edge.

Numerical integration, with uniformly spaced increments across a linear aperture, is a weighted sampling. Equation 4 gives the fold-over point in the k-space pattern for this sampling, as well. The errors of numerical integration are related to the derivative, to an order depending on the order of the Newton-Cotes method and the sample size. For a linear aperture, we can find the distribution of the errors for numerical integration. The results above can be interpreted as the errors from a pulse integration.

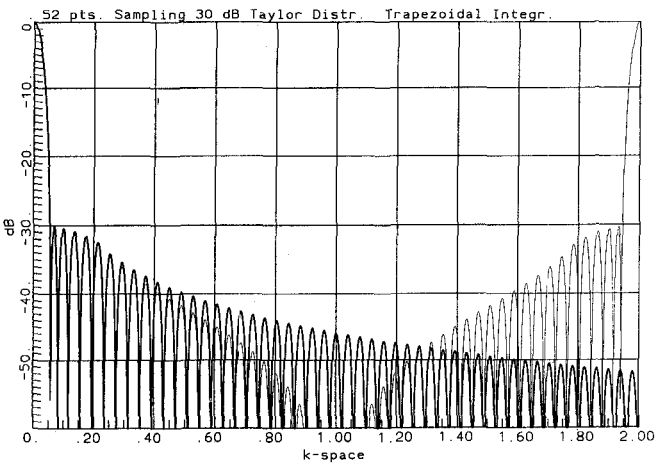

Figure 9. A comparison between the patterns obtained using exact integration (dark curve) and trapezoidal integration (light curve) for an aperture distribution with an edge-step discontinuity.

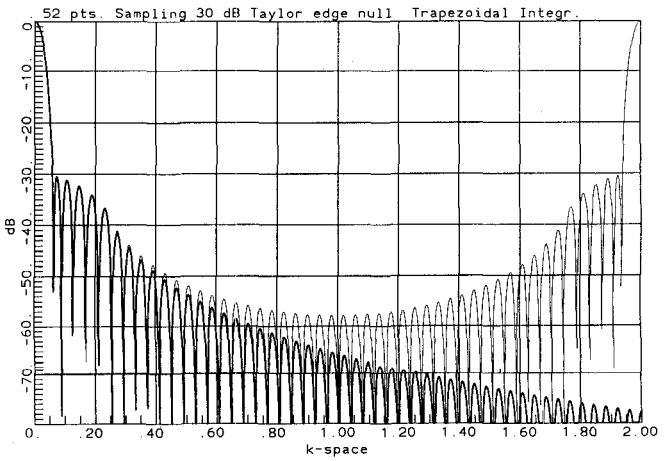

Figure 10. The same comparison as shown in Figure 9, for an aperture distribution with a linear slope at the edge.

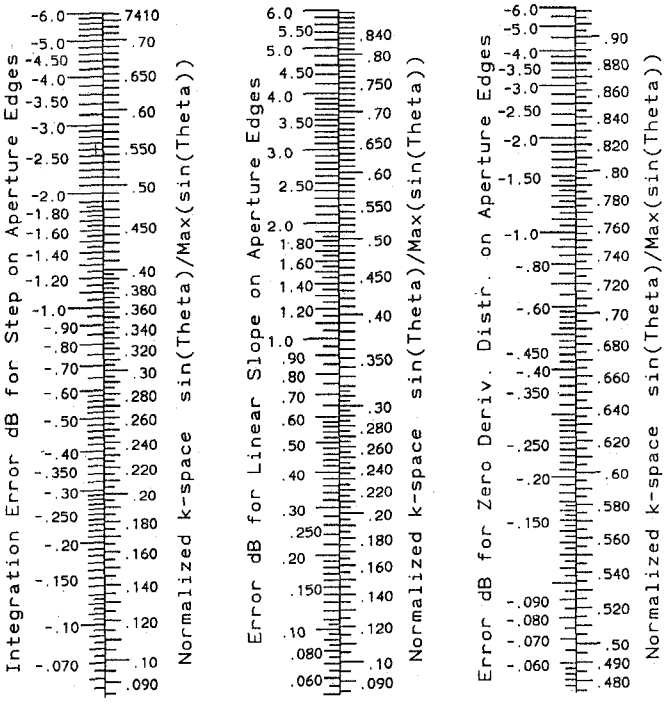

Figure 11. A nomograph giving the error that results from using trapezoidal integration for three aperture distributions.

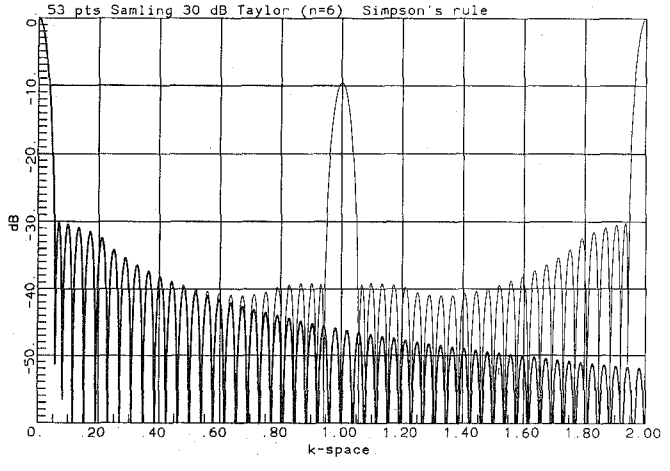

Figure 12. The comparison shown in Figure 9, but with the integration done using Simpson's rule.

Figure 9 gives the comparison between the exact integration (dark), and the use of trapezoidal integration (light), on an aperture with an edge-step discontinuity. A comparison of this plot with Figure 4 shows that the errors have the opposite sense. Figure 10 continues the development, with an aperture distribution with a linear slope at the edge. Using these results, Figure 11 gives a nomograph for the errors of trapezoidal integration on a linear aperture. The error depends on the normalized distance from the fold-over point and the edge condition on the aperture.

The analysis was extended to Simpson's rule. Figure 12 repeats the results of Figure 9. This pattern shows a large error at the fold-over point. This is due to the inner sampling weights of 4, 2, 4, 2, ..., 2, 4, a sampling at twice the spacing of the uniformly weighted trapezoidal integration in the central portion. Figure 13, for the aperture with a linear slope on the edge, shows the same characteristic as Figure 12. The distance from the fold-over point is more restricted for the Simpson's-rule integration. Figure 14 is a nomograph for the error distribution of the Simpson's-rule integration for the three aperture edge conditions.

References

1. T.T. Taylor, "Design of Line Source Antennas for Narrow Beamwidth and Low Sidelobes," *IEEE Transactions on Antennas and Propagation*, **AP-4**, 1, January 1955, pp. 16-28.

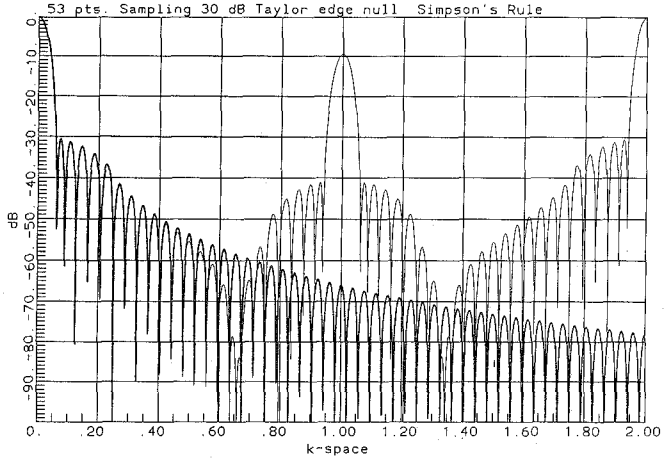

Figure 13. The comparison shown in Figure 10, but with the integration done using Simpson's rule.

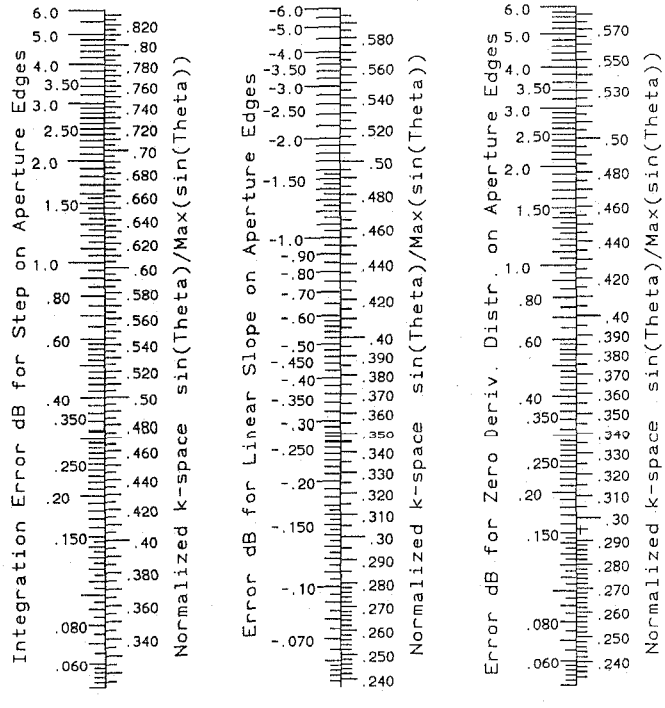

Figure 14. A nomograph giving the error that results from using Simpson's-rule integration for three aperture distributions.

2. D. R. Rhodes, "On the Taylor Distribution," *IEEE Transactions on Antennas and Propagation*, **AP-20**, 2, March 1972, pp. 143-145.

3. D. R. Rhodes, "On a New Condition for Physical Realizability of Planar Antennas," *IEEE Transactions on Antennas and Propagation*, **AP-19**, 2, March 1971, pp. 162-166.

Further Comments

A discussion with W. Neill Kefauver, the manager of the Lockheed Martin near-field facility in Denver, about the sampling requirements gave insights into a practical approach to determining measurement errors. The aperture plane is normally over-sampled, when we consider the sidelobes near boresight. When every other point is removed, a FFT can still produce the pattern. A comparison of the prediction of the sidelobes for these two cases gives a measure of the error. The analysis can be continued by again removing every other point, to give another point which leads to a curve of error versus sampling interval at this point, off boresight.

Ideas for Antenna Designer's Notebook

Ideas are needed for future issues of the *Magazine*. Please send your suggestions to Tom Milligan and they will be considered for publication as quickly as possible. Topics can include antenna design tips, equations, nomographs, or shortcuts as well as ideas to improve or facilitate measurements.

Special Offer to Contributors

How would you like a complete set of the Antenna Designer's Notebook articles published since this column began, in the August, 1983, issue? Send an idea which is used for a future issue of our Notebook to Tom Milligan, and you will be rewarded with a notebook containing copies of all items, **including yours,** when it is published. This column is a **great opportunity** for many of our AP-S members who are too busy to publish a lengthy paper, but who would like to share some **practical information** which can help to increase the productivity of the antenna and propagation engineers.

Updated Table of Contents

An updated Table of Contents for the Antenna Designer's Notebook was published in the August, 1983, issue of the *Magazine*.

Report on the 1997 Wireless Communications Conference

Keywords: conference; wireless telecommunications; radio frequency; microwave; broadband; nonlinearity; power amplifier; antennas; propagation; Local Multipoint Distribution Service; integrated passive components

1. Abstract

This conference report reviews the 1997 Wireless Communications Conference, which was held in Boulder, Colorado, August 11-13, 1997. The report emphasizes the contributions of the conference in technology areas including broadband telecommunications systems, radio-frequency devices and components, nonlinear effects, and propagation.

2. Introduction

Wireless telecommunications systems, exploiting the air as a transmission medium, provide portability and are increasingly taking the place of wired systems, even for fixed terminals. However, the air is a shared medium. Compatibility and standards problems are central to the technological issues faced by this industry. In many countries, notably the United States, wireless communications licenses are being awarded without strict reference to their use and without interoperability standards. The result is a somewhat chaotic state in which many transmission standards coexist. Without government to dictate standards, systems operators must make independent decisions, based largely on technological grounds, concerning their equipment standards. The wisdom of such decisions depends, to large extent, on the quality and detail of technical data available about proposed systems.

The desire to explore some of the finer details of wireless systems was behind the first Wireless Communications Conference, held in Boulder, Colorado, in 1996. The great response to this conference led directly to the 1997 Wireless Communications Conference (WCC'97), also held in Boulder, August 11-13, 1997. WCC'97 was sponsored by the IEEE Microwave Theory and Techniques Society and by the International Microelectronics and Packaging Society (IMAPS). Technical co-sponsors of the event were the National Institute of Standards and Technology (NIST), the Institute for Telecommunications Sciences (ITS), and the IEEE Communications Society. 254 people registered for the conference, an increase of about 50% from 1996. Attendees came from 14 nations: Austria, Belgium, Canada, Finland, France, Germany, Israel, Japan, Korea, the Netherlands, Spain, Switzerland, the United Kingdom, and the United States; 42 registrants were from outside the United States. Both the 1996 and 1997 conferences were chaired by Dr. Roger Marks, of NIST.

One of the essential features of the conference was that offered a deep view of the industry, from high-level issues, such as systems, to low-level topics, such as components, in a single-track format. As a result, it brought together customers and suppliers throughout the supply chain, in an interactive format. Attendees voiced their approval of this opportunity to see the big picture, and to help address the many wireless-communications problems that require an interdisciplinary approach.

3. Technical sessions

The technical program was overseen by the Technical Chair, Dr. Michael S. Heutmaker, of Lucent Technologies, along with an international Technical Program Committee of 23 members. From 81 submitted manuscripts from 17 countries, this committee selected 51 for oral presentations. These were arranged in ten sessions:

Local Multipoint Distribution System (LMDS) was chaired by Mohammad Shakouri, of Hewlett-Packard. LMDS is a wireless system, providing broadband digital access for video, voice, and data to homes and business. The system has received a great deal of attention abroad. Furthermore, with the United States' Federal Communications Commission (FCC) having recently allocated over 1 GHz of bandwidth, between 27.5 GHz and 31.3 GHz, for such services, many of the major telecommunications players are rushing to establish themselves in this potentially huge marketplace. The session included papers covering system issues, propa-